Analysis of Surface Temperature on Welding Plates using Aggressive Liquid Cooling

Muhammad Abdullah Zafar Ghauri[a]

[a]School of Mechanical and Manufacturing Engineering (SMME), National University of Sciences and Technology (NUST), Islamabad, H-12, 44000, Pakistan

mghauri.ug22smme@student.nust.edu.pk

25st April 2025

Abstract

This study presents a comprehensive analysis of surface temperature distribution in welding plates subjected to aggressive liquid cooling. A steady-state, two-dimensional heat conduction model is developed using the separation of variables method to solve the governing Laplace equation with non-homogeneous boundary conditions. The problem involves a plate with clamped edges maintained at constant surface temperature, a position-dependent heat flux at the top surface, and liquid jet cooling at the bottom. The solution is obtained using eigenfunction expansion and orthogonality principles, implemented computationally to evaluate temperature profiles and contour plots. The results demonstrate the effectiveness of aggressive cooling in controlling temperature gradients near the weld joint, with significant implications for thermal management in welding processes.

Keywords: surface temperature distribution, aggressive liquid cooling, jet cooling, temperature gradient, thermal management

1 Problem Statement

One is evaluating a technique for controlling the properties of welded joints by using aggressive liquid cooling.The following Figure 1 illustrates a cut-away view of two plates that are being welded together. Both edges of the plate are clamped and effectively held at temperatures $T_s = 25^oC$. The top of the plate is exposed to a heat flux that varies with position x, measured from joint, according to: $\dot{q}^{"}_m(x) = \dot{q}^{"}_j e^{\frac{-x}{L_j}}$ where $\dot{q}^{"}_j = 1 * 10^6 W/m^2$ is the maximum heat flux (at the joint, x = 0) and and $L_j = 2.0\,cm.$ is a measure of the extent of the heat flux. The back side of the plates are exposed to aggressive liquid cooling by a jet of fluid at $T_f = -35^oC$ with $\bar{h} = 5000 W/m^2K$. A half-symmetry model of the problem is shown in Figure 1. The thickness of the plate is $b = 3.5$ cm and the width of a single plate is $W = 8.5$ cm. You may assume that the welding process is steady-state and 2-D. You may neglect convection from the top of the plate. The conductivity of the plate material is $k = 38 W/mK$ Nellis and Klein (2009).

1. Develop a separation of variables solution to the problem. Implement the solution in EES and prepare a plot of the temperature as a function of x at y = 0, 1.0, 2.0, 3.0, and 3.5 cm.
2. Prepare a contour plot of the temperature distribution.

Solution

1.1 1.

The follwoing problem is governed by following differetial equation, which is the typical Laplacian equation of heat modelling:

$$\frac{\partial^2 T}{\partial x^2} + \frac{\partial^2 T}{\partial y^2} = 0 \tag{1}$$

The boundary conditions corresponding to 1 are:

$$\frac{\partial T}{\partial x}_{x=0} = 0 \tag{2}$$

$$T_{x=W} = T_s \tag{3}$$

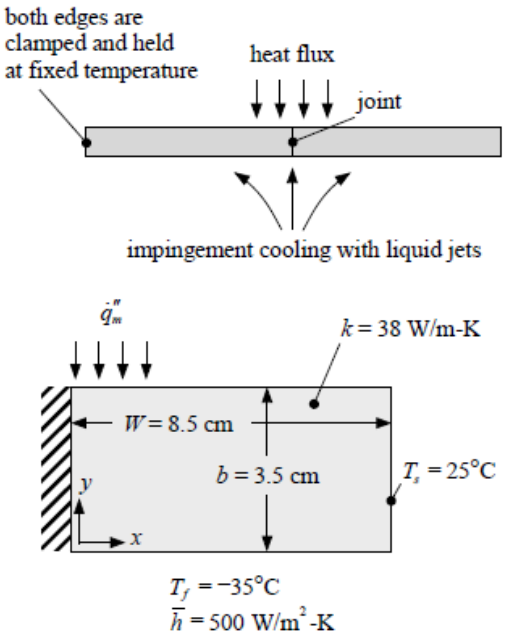


Figure 1: Welding process and half-symmetry model of the welding process.

$$k\frac{\partial T}{\partial y}_{y=0} = h(T_{y=0} - T_f) \tag{4}$$

$$k\frac{\partial T}{\partial y}_{y=0} = \dot{q}''_m \tag{5}$$

The governing differential equation 1 has three non-homogeneous boundary conditions and hence the solution cannot be evaluated suing separation of variables . By transformation, the solution can be evaluated:

$$\theta = T - T_s \tag{6}$$

transforms the boundary condition at $x = W$to a homogeneous boundary condition and provides a homogeneous direction (x). The transformed differential equation and boundary conditions are:

$$\frac{\partial^2\theta}{\partial x^2} + \frac{\partial^2\theta}{\partial y^2} = 0 \tag{7}$$

and has boundary conditions as

$$\frac{\partial\theta}{\partial x}_{x=0} = 0 \tag{8}$$

$$\theta_{x=W} = 0 \tag{9}$$

$$k\frac{\partial\theta}{\partial y}_{y=0} = h(\theta_{y=0} - \theta_f) \tag{10}$$

$$k\frac{\partial\theta}{\partial y}_{y=0} = \dot{q}''_m \tag{11}$$

where

$$\theta_f = T_f - T_s \tag{12}$$

The separated solution is assumed to be:

$$T = TXTY \tag{13}$$

When substituted in 7, the process results in two ordinary differential equations as:

$$\frac{d^2TX}{dx^2} + \lambda^2 TX = 0 \tag{14}$$

$$\frac{d^2TY}{dy^2} - \lambda^2 TY = 0 \tag{15}$$

The solutions corresponding to 14 and 15 are as follows:

$$TX = C_1 sin(\lambda x) + C_2 cos(\lambda x) \tag{16}$$

$$TY = C_3 sin(\lambda y) + C_4 cos(\lambda y) \tag{17}$$

The solution is initiated in homogeneous direction initially (which corresponds to the eigenproblem). The boundary condition x=0, when implemented on 8 results in:

$$\frac{dTX}{dx}_{x=0} = [C_1 \lambda cos(\lambda x) - C_2 \lambda sin(\lambda x)]_{x=0} = C_1 \lambda = 0 \tag{18}$$

Since $C_1 = 0$, therefore:

$$TX = C_2 (cos \lambda x) \tag{19}$$

With boundary condition at $x = W$, 9 results in:

$$TX_{x=W} = C_2 (cos \lambda W) = 0 \tag{20}$$

Eigenvalues are evaluated from 20 as:

$$\lambda_i = \frac{(1+2i)\pi}{2W} \qquad \forall \quad i = 1, 2, \ldots, \infty \tag{21}$$

and the eigenfunction are:

$$TX_i = C_{2,j} cos(\lambda_i x) \tag{22}$$

The solution for TX is the sum of the eigenfunctions:

$$TX = \sum_{i=0}^{\infty} C_{2,i} \cos(\lambda_i x) \tag{23}$$

and the solution for the temperature is:

$$TX = \sum_{i=0}^{\infty} C_{2,i} \cos(\lambda_i x) \left[C_{3,i} \sinh(\lambda_i y) + C_{4,i} \cosh(\lambda_i y)\right] \tag{24}$$

Note that $C_{2,i}$ can be absorbed in the other constants:

$$\theta = \sum_{i=0}^{\infty} \cos(\lambda_i x) \left[C_{3,i} \sinh(\lambda_i y) + C_{4,i} \cosh(\lambda_i y)\right] \tag{25}$$

Equation (25) is substituted into the boundary condition at $y = 0$, Eq. (10):

$$k \sum_{i=0}^{\infty} \cos(\lambda_i x) \left[C_{3,i} \lambda_i \cosh(\lambda_i 0) + C_{4,i} \lambda_i \sinh(\lambda_i 0)\right] = h \left\{ \sum_{i=0}^{\infty} \cos(\lambda_i x) \left[C_{3,i} \sinh(\lambda_i 0) + C_{4,i} \cosh(\lambda_i 0)\right] - \theta_j \right\} \tag{26}$$

or

$$k \sum_{i=0}^{\infty} \cos(\lambda_i x) \, C_{3,i} \lambda_i = h \left[\sum_{i=0}^{\infty} \cos(\lambda_i x) \, C_{4,i} - \theta_j \right] \tag{27}$$

We take advantage of the orthogonality of the eigenfunctions by multiplying Eq. (27) by an arbitrary eigenfunction and integrating from $x = 0$ to $x = L$ in order to achieve:

$$k C_{3,i} \lambda_i^4 \int_0^W \cos^2(\lambda_i x) \, dx = h \left\{ C_{4,i} \int_0^W \cos^2(\lambda_i x) \, dx - \theta_f \int_0^W \cos(\lambda_i x) \, dx \right\} \tag{28}$$

which leads to:

$$\frac{k C_{3,i} \lambda_i W}{2} = h \left[\frac{C_{4,i} W}{2} - \theta_f \frac{2(-1)^i W}{(1+2i)\pi} \right] \tag{29}$$

or

$$\theta_f \frac{4(-1)^i}{(1+2i)\pi} = C_{4,i} - \frac{k \lambda_i}{h} C_{3,i} \tag{30}$$

which is one equation for each of the two pairs of unknown coefficients.
Equation 25 and are substituted into the final boundary condition at $y = b$, Eq. (11):

$$k \sum_{i=0}^{\infty} \cos(\lambda_i x) \left[C_{3,i} \lambda_i \cosh(\lambda_i b) + C_{4,i} \lambda_i \sinh(\lambda_i b)\right] = q_j'' \exp\left(-\frac{x}{L_j}\right) \tag{31}$$

Again, the orthogonality of the eigenfunctions is used to obtain:

$$k\left[C_{3,i}\lambda_i\cosh\left(\lambda_i b\right)+C_{4,i}\lambda_i\sinh\left(\lambda_i b\right)\right]\int_0^W\cos^2\left(\lambda_i x\right)dx=q_j''\int_0^W\exp\left(-\frac{x}{L_j}\right)\cos\left(\lambda_i x\right)dx \tag{32}$$

or

$$C_{3,i}\lambda_i\cosh\left(\lambda_i b\right)+C_{4,i}\lambda_i\sinh\left(\lambda_i b\right)=\frac{2q_j''}{Wk}\int_0^W\exp\left(-\frac{x}{L_j}\right)\cos\left(\lambda_i x\right)dx \tag{33}$$

which is the 2nd relationship between the coefficient pairs. The integral on the right-hand side of Eq. (33) is accomplished using Maple as:

```
> restart;
> assume(i,integer);
> lambda:=(1+2*i)*Pi/(2*W);
```

$$\lambda := \frac{(1+2i\sim)\pi}{2W} \quad (1)$$

```
> int((cos(lambda*x))^2,x=0..W);
```

$$\frac{W}{2} \quad (2)$$

```
> int(cos(lambda*x),x=0..W);
```

$$\frac{2(-1)^{i\sim}W}{(1+2i\sim)\pi} \quad (3)$$

```
> int(exp(-x/L_j)*cos(lambda*x),x=0..W);
```

$$\frac{2L_jW\left(2L_j\pi(-1)^{i\sim}e^{-\frac{W}{L_j}}i\sim+L_j\pi(-1)^{i\sim}e^{-\frac{W}{L_j}}+2W\right)}{4L_j^2\pi^2i\sim^2+4L_j^2\pi^2i\sim+L_j^2\pi^2+4W^2} \quad (4)$$

Figure 2: Maple Code for Evaluation of Integrals

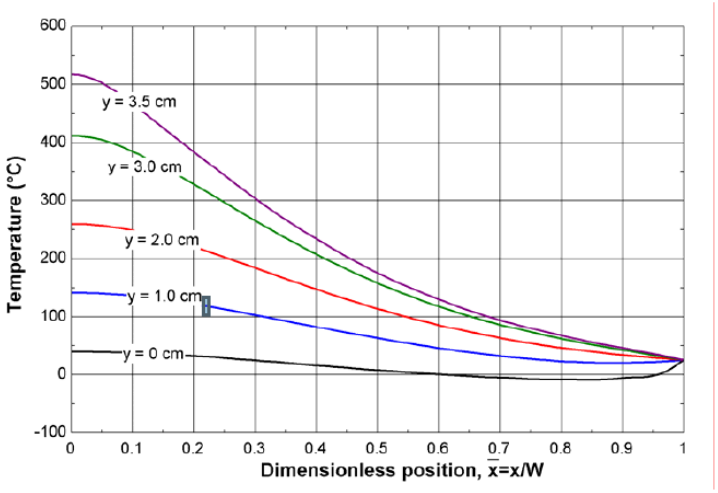


Figure 3: Temperature as a function of x/W for various values of y.

```
    $UnitSystem SI MASS RAD PA K J
$TABSTOPS 0.2 0.4 0.6 0.8 3.5 in
"Inputs"
b=3.5 [cm]*convert(cm,m) "plate thickness"
W=8.5 [cm]*convert(cm,m) "plate width"
k=38 [W/m-K] "plate conductivity"
T_s=converttemp(C,K,25) "edge temperature"
T_f=converttemp(C,K,-35) "fluid temperature"
h=5000 [W/m^2-K] "heat transfer coefficient"
q=1e6 [W/m^2] "heat flux at x=0"
L_j=2.0 [cm]*convert(cm,m) "extent of the heat flux"
"Position"
"x_bar=0.5"
x=x_bar*W
"y_bar=0.5"
y=y_bar*b
N=10 [-] "number of terms"
theta_f=(T_f-T_s) "transformed fluid temperature"
Duplicate i=0,N
```

```
lambda[i]=(1+2*i)*pi/(2*W)
theta_f*4*(-1)^i/((1+2*i)*pi)=C_4[i]-k*lambda[i]*C_3[i]/h
C_3[i]*lambda[i]*cosh(lambda[i]*b)+C_4[i]*lambda[i]*sinh(lambda[i]*b)=(2*q/(W*k))*(2*W*
    L_j*(2*W*exp(W/L_j)+Pi*L_j*(-1)^i+2*Pi*L_j*(-1)^i*i)*exp(-W/L_j)/(4*W^2+Pi^2*L_j^2+4*
    Pi^2*L_j^2*i+4*Pi^2*L_j^2*i^2))"Maple Solution"
theta[i]=cos(lambda[i]*x)*(C_3[i]*sinh(lambda[i]*y)+C_4[i]*cosh(lambda[i]*y))
theta[i]=cos(lambda[i]*x)*(C_3[i]*sinh(lambda[i]*y)+C_4[i]*cosh(lambda[i]*y))
End
T=T_s+sum(theta[0..N])
T_C=converttemp(K,C,T)
```

Listing 1: EES Code for Numerical Evaluation of Solution



Figure 4: Contour plot of the temperature distribution in the plate.

Conclusion

The analysis successfully demonstrates the application of separation of variables to solve a two-dimensional heat conduction problem with multiple non-homogeneous boundary conditions in welding plates. The transformation technique effectively homogenizes the boundary conditions, enabling the use of eigenfunction expansions. The computational implementation yields detailed temperature distributions, revealing that aggressive liquid cooling maintains the plate temperature within acceptable limits despite the high heat flux at the weld joint. The contour plots visually confirm the expected temperature gradients, with maximum temperatures occurring near the joint and effective cooling at the plate boundaries. This work provides valuable insights for optimizing welding processes through controlled cooling strategies, with potential applications in industrial manufacturing where thermal distortion must be minimized. Future work could extend this approach to transient analyses or three-dimensional configurations.

References

Nellis, G., & Klein, S. (2009). *Heat transfer* (1st ed.). Cambridge University Press.